2023 IEEE/ASME International Conference on Advanced Intelligent Mechatronics (AIM)
June 28-30, 2023. Seattle, Washington, USA

Predictive Assistive Motion Generation Based on Human Intent for Human-Collaborative Robots

Naoki Ichimura and Jun Ishikawa, *Member, IEEE*

***Abstract*— In this paper, a method is proposed to estimate the velocity of the hand cooperating with the robot as human intent based on human surface electromyography signals, and to make the robot move in a predictive assistive motion. Specifically, an index to measure the matching index between human hand velocity and robot motion is proposed, based on the estimation of human hand velocity from human surface electromyography signals by a recurrent neural network, and using this as the human intent. Furthermore, the strength of the robot's support is adjusted based on the matching index to achieve predictive assistive motion behavior of the robot during cooperative work. In the experiment, an index to measure the burden of human work was defined, and the effectiveness of the proposed method was verified. Specifically, the proposed method was implemented and evaluated for the task of manipulating an object in cooperation with an impedance-controlled robot. The results show that the proposed method can reduce the burden on humans.**

I. Introduction

In recent years, concepts have been proposed to promote change in manufacturing and society. Industry 4.0, advocated by Germany, aims to establish flexible production systems, such as autonomous decentralized manufacturing and variable-type, variable-volume production, through the use of IT technology and digital data [1]. In addition, Society 5.0 proposed by Japan aims to realize a smart society that balances economic development and the resolution of social issues through the use of IoT technology, AI, and other applications [2]. In order to realize such flexible and smart factories, robots are being introduced. In particular, the introduction of human-collaborative robots is being promoted in line with the relaxation of the 80W regulation, and is intended to solve social issues such as reducing the burden on humans.

Impedance control is commonly used as a method to achieve cooperative behavior between robots and humans [3]. In impedance control, when the parameters of the impedance model are set to large values, the human-load is increased because the human must exert a large amount of force to operate the robot. In contrast, when the parameters of the impedance model are set to small values, the force required to operate the robot is smaller and the human-load is reduced, but there is a problem of reduced stability when in contact with a hard environment [4][5]. Therefore, many studies have been conducted to ensure the stability of impedance control [6][7][8].

Many studies have also been conducted to achieve cooperative behavior with humans without using impedance control. A method utilizing Series Elastic Actuator (hereinafter referred to as SEA) [9] has been proposed as a previous study to reduce human-load by using a robot that works in cooperation with humans [10][11][12]. In these studies, the deflection of the SEA is properly controlled to improve the back drivability of the robot, thereby reducing the force exerted by the human during robot operation. In addition, a method utilizing human surface electromyography signals (hereinafter referred to as iEMG signals) has also been proposed [13][14][15]. In these studies, torque is calculated from the measured iEMG signals to operate the exoskeleton and assist the human to reduce human-load. Other methods have been proposed to reduce the human-load by dividing roles between humans and robots [16], and to reduce the human-load by learning actions in the repetition of the same operations [17]. The above research is a method of assisting humans and reducing human-load by having the robot act passively.

In this study, a method is proposed to reduce the human-load by making the robot move in a predictable manner. The proposed method takes advantage of the fact that the iEMG signal is output about 0.1 s earlier than the actual body motion. An attempt is made to reduce human-load by estimating human intent from the iEMG signal and allowing the robot to operate predictably. In addition, an evaluation index to evaluate the matching index between human intent and predictive assistive motion and an evaluation index to evaluate human-load are defined, respectively, to verify the effectiveness of the predictive assistive motion using the proposed method.

In the following, a control system for predictive assistive motion is first described, together with the configuration of the recurrent neural network (RNN) used in the system. Next, the definitions of the evaluation indexes for "matching index between human intent and predictive assistive motion" and "human-load" are described. Furthermore, the effectiveness of the proposed method is confirmed based on an evaluation index defined from the results of actual operations with the implementation of the proposed method.

II. Predictive Assistive Motion Generation Based on Human Intent

In this chapter, a control system for human-collaborative robots to realize predictive assistive motion is proposed.

A. Configuration of Control System for Predictive Assist

In this section, a method for constructing a control system to realize predictive assistive motion in a robot is proposed. This study targets a task in which a human manipulates the tip of the robot to move it in only one direction (X-axis direction).

N. Ichimura and J. Ishikawa are with the Department of Robotics and Mechatronics, Tokyo Denki University, 5 Senju Asahi-cho, Adachi-ku, Tokyo 120-8551, Japan (Phone: +81-3-5284-5607; fax: +81-3-5284-5698, email: ishikawa@fr.dendai.ac.jp).

Fig. 1 shows the configuration of the control system to realize the proposed predictive assistive motion. The control target, i.e., the robot, is position-controlled in a Cartesian coordinate system by the Equipped controller. The proposed control system is then composed of a passive motion generator shown in the green dashed box and a predictive assistive motion generator shown in the red dashed box.

The predictive assistive motion generator uses the fact that the human iEMG signal ($iEMG_1$, $iEMG_2$) is output about 0.1 s earlier than the actual body motion to estim ate the velocity of the human hand $\hat{v}_{hand}$ [m/s] 0.1 s ahead from the iEMG signal ($iEMG_1$, $iEMG_2$). Hand velocity is estimated using an RNN, which will be described in the next section.

Then, the position command $\hat{x}_{hand}$ [m] of the predictive assistive motion is generated by applying the adjustment gain calculated based on the "matching index between human intent and predictive assistive motion" described in Section 3.1 to the estimated hand velocity $\hat{v}_{hand}$, passing it through a drift prevention high-pass filter, and integrating it.

Then, the force f [N] applied by the human to the robot drives the impedance model, which is the passive motion part, and the position output x_d [m] and the position command of the predictive assistive motion $\hat{x}_{hand}$ are added together to form the position command x_{ref} [m] to the robot.

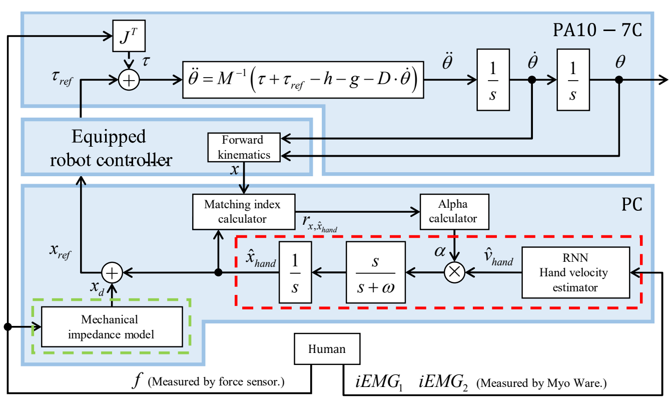

Figure 1. Block diagram of proposed control system for generating predictive motion: Adjustment is made by multiplying the estimated velocity by the Adjustment gain calculated from the matching index.

B. RNN Configuration for Estimating Human Hand Velocity

In this section, an RNN configuration used to estimate the velocity of a human hand from iEMG signals is described. In this study, the velocity of a human hand is estimated from two iEMG signals ($iEMG_1$, $iEMG_2$). The iEMG signals of channel 1 and channel 2 ($iEMG_1$, $iEMG_2$) are input as feature vectors, and the RNN is trained with the hand velocity as the output teaching signal. Fig. 3 shows the RNN configuration used. As shown in Fig. 3, $x[k]$ is the feature vector for RNN, and is expressed as

$$\boldsymbol{x}[k]=\begin{bmatrix} iEMG_1[k] \\ iEMG_2[k] \end{bmatrix} \tag{1}$$

by combining the iEMG signal of channel 1 and the iEMG signal of channel 2 ($iEMG_1$, $iEMG_2$). Also, as shown in Fig. 3, the output of RNN is the velocity of a human hand, which is calculated by

$$h_N[k]=\sigma_t\left(b_h+W_x\cdot\boldsymbol{x}_N[k]+W_h\cdot\left[h_N[k-1]^T,h_N[k-2]^T,\cdots h_N[k-N]^T\right]\right)^T \tag{2}$$

$$y_N[k]=b_0+W_0\cdot h_N[k] \tag{3}$$

In equations (2) and (3), N is the number of tap delays in the RNN, and in this study, $N=5$. Also, the number of nodes in the hidden layer was set to 13. Tap delay and the number of hidden layers were determined by trial and error. The activation function of the hidden layer is the hyperbolic tangent sigmoid transfer function $\sigma(u)$, and the activation function of the output layer is the linear transfer function.

Fig. 2 shows the structure of the feature vectors and teacher signal data to be trained by the RNN. In this study, to estimate the hand velocity $\hat{v}_{hand}$ 0.1 s ahead from the iEMG signal ($iEMG_1$, $iEMG_2$), data of the hand velocity v_{hand} is offset by 0.1s from the iEMG signal data as shown in Fig. 2. Since the sampling time in robot control is 10 ms, this time an offset of 0.1s is made by adding 10 data "0".

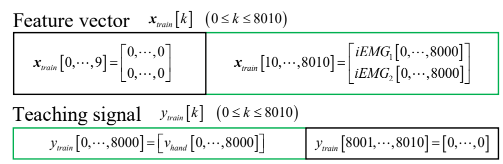

Figure 2. Structure of input (feature vector) and output (teaching signal) for training of recurrent neural network.

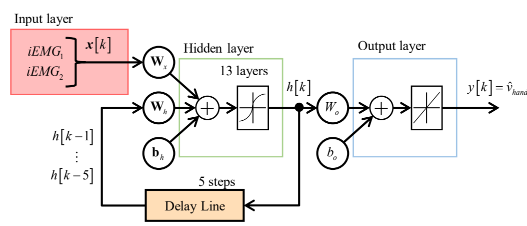

Figure 3. Structure of recurrent neural network to estimate human hand velocity from iEMG signals.

III. Definition of Evaluation Index

Predictive assistive motion aims to reduce the human-load in robot operation by estimating human intent and making the robot move. This chapter defines an evaluation index to quantitatively evaluate the effectiveness of the proposed predictive assistive motion. Specifically, two evaluation indexes are proposed: "matching index between human intent and predictive assistive motion" and "human-load".

A. Matching Index Between Human Intent and Predictive Assistive Motion

In this section, the definition of matching index between human intent and predictive assistive motion (hereinafter referred to as "matching index") and the calculation method of the evaluation index are explained. In this study, it is assumed that the position of the object (hereinafter referred to as baton) to be manipulated in cooperation with the robot can be manipulated as intended by the human intent. The position of the baton is treated as "human intent" and the integral of the estimated hand velocity is treated as "predictive assistive motion" to define the evaluation index.

Specifically, the correlation coefficient between the baton position and the integral of the hand velocity estimate is used as a matching index.

However, for averaging an appropriate moving window is adopted, the correlation coefficient is calculated for that range. To further adjust for the effects of changes over time and to improve the response to changes in the baton position and the integral of the hand velocity estimate , a forgetting factor is introduced. The proposed matching index is defined as

$$r_{x,\hat{x}_{hand}}[k] = \frac{S_{x,\hat{x}_{hand}}[k]}{S_x[k]\cdot S_{\hat{x}_{hand}}[k]} \tag{4}$$

However, $S_{x,\hat{x}_{hand}}$, S_x, and $S_{\hat{x}_{hand}}$ represent the covariance of the baton position x and the integral of the hand velocity estimate $\hat{x}_{hand}$, the standard deviation of the baton position x, and the standard deviation of the integral of the hand velocity estimate $\hat{x}_{hand}$, respectively, and are calculated according to

$$S_{x,\hat{x}_{hand}}[k] = \frac{1}{G}\sum_{i=k-n+1}^{k}\left(g_{k-i}\cdot x[i]-\overline{x}[k]\right)\left(g_{k-i}\cdot \hat{x}_{hand}[i]-\overline{\hat{x}}_{hand}[k]\right) \tag{5}$$

$$S_x[k] = \sqrt{\frac{1}{G}\sum_{i=k-n+1}^{k}\left(g_{k-i}\cdot x[i]-\overline{x}[k]\right)^2} \tag{6}$$

$$S_{\hat{x}_{hand}}[k] = \sqrt{\frac{1}{G}\sum_{i=k-n+1}^{k}\left(g_{k-i}\cdot \hat{x}_{hand}[i]-\overline{\hat{x}}_{hand}[k]\right)^2} \tag{7}$$

Also, n represents the number of samples in the window width, and $\overline{x}[k]$ and $\overline{\hat{x}}_{hand}[k]$ are the weighted average values of the baton position x and the integral of the hand velocity estimate $\hat{x}_{hand}$ within the window width, respectively, which are calculated by

$$\overline{x}[k] = \frac{1}{G}\sum_{i=k-n+1}^{k} g_{k-i}\cdot x[i] \tag{8}$$

$$\overline{\hat{x}}_{hand}[k] = \frac{1}{G}\sum_{i=k-n+1}^{k} g_{k-i}\cdot \hat{x}_{hand}[i] \tag{9}$$

Also, g_i is the forgetting factor and G is the sum of the forgetting factors.

B. Evaluation Index of Human-load

In this section, the definition of the human-load and the calculation method of the evaluation index are explained. In this study, human-load is defined as a physical quantity related to the work done by humans, specifically, the integral value of a hypothetical fictitious power as an evaluation index (hereinafter referred to as human-load index).

Specifically, the fictitious power calculated from the force f applied by the human to the robot and the velocity $\dot{x}_d$ of the output of the impedance model x_d is defined as in

$$P[k] = f[k]\cdot \dot{x}_d[k] \tag{10}$$

The human-load index is defined as the integral of the fictitious power as a measure of human-load.

The reasons for using virtual power in the computation of the human-load index are explained here. In this study, human-load is considered to be applying force by the human during the operation of the PA10. Therefore, it is necessary to avoid a power of 0 Nm/s in the state in which the human is emitting force. Suppose that the power P' is defined as

$$P'[k] = f[k]\cdot \dot{x}[k] \tag{11}$$

using the force applied by the human f to the robot and the velocity of the baton $\dot{x}$. In the proposed method, the position command x_{ref} is determined by adding the position output of the impedance model x_d and the position command of the predictive assistive motion $\hat{x}_{hand}$. Therefore, it is possible that $\dot{x}_d = -\dot{\hat{x}}_{hand}$, in which case the position output of the impedance model x_d and the position command of the predictive assistive motion $\hat{x}_{hand}$ cancel each other out, so the baton position x remains unchanged and the power becomes $P' = 0$ N/m/s regardless of the force applied by the human f to the robot. Therefore, the virtual power is calculated from the force applied by the human f to the robot and the velocity $\dot{x}_d$ of the position output x_d of the impedance model, as shown in Equation (10). Since the impedance model is driven while a human applies a force to the robot, $\dot{x}_d$ is not to be zero if $f \neq 0$. This means that a power of 0 Nm/s can be avoided in the state where the human is emitting force.

The position generated by the impedance model can also be interpreted as the difference between human intent (resulting baton position) and predictive assistive motion.

IV. Preliminary Experiments for RNN Training

In this chapter, the results of acquiring iEMG signals and human hand velocity during baton manipulation through experiments and training them to RNN are described.

A. Experimental Setup

Fig. 4 shows the system configuration of the experimental apparatus. Fig. 5 shows the configuration of the experimental apparatus used in this study.

As shown in these figures, the experimental apparatus consisted of an industrial manipulator PA10-7C (hereafter referred to as PA10) with a force sensor and an aluminum baton for manipulation fixed at the tip, and a MyoWare myoelectric sensor attached to the operator's arm. The EMG sensors are attached to the biceps brachii and triceps brachii, channel 1 ($iEMG_1$) and channel 2 ($iEMG_2$), respectively. The measured iEMG signals are sent to the PC via Arduino UNO and Arduino DUE with the wireless module Xbee. In addition, the iEMG signals are also displayed on an oscilloscope to verify that they are acquired correctly during the experiment.

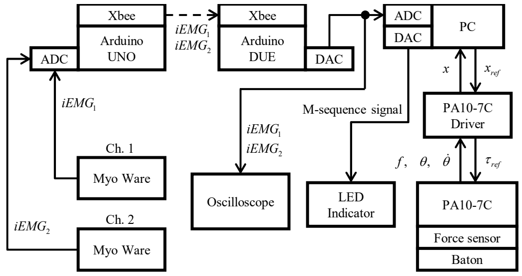

Figure 4. Schematic diagram of experimental system configuration.

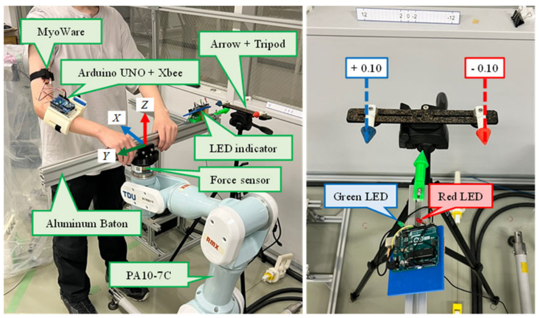

Figure 5. Experimental setup that consists of a manipulator with a 6-axis force sensor, myoelectric sensors, and LED indicator.

B. Experimental Procedure

This section describes the procedure for acquiring iEMG signals and velocity data of the hand grasping the baton during manipulator operation.

As shown in Fig. 5 in the previous section, prepare two arrows (red and blue) attached to a tripod as well as an arrow (green) attached to the end of the baton attached to the tip of the PA10. The two arrows on each of the tripod are positioned ±0.1 m from the baton's origin in the X-axis direction, and the operator manipulates the baton within this range. The baton is operated according to the operation instructions based on the previously generated M-sequence signals. The fundamental period of the M-sequence signal was set to 1 Hz and generated by the generator $z^{24}+z^{23}+z^{22}+z^{17}+1$. The M-sequence signal was sampled with a sampling period of 0.9 s and a normally distributed sampling fluctuation (jitter) with a standard deviation of 0.08 s at an integer multiple of 10 ms, the control period.

Operation instructions by M-sequence signals are transmitted to the operator by LED indicators. The operator aligns the arrow (green) attached to the baton with the blue arrow when the green LED is lit and with the red arrow when the red LED is lit. The baton operation time in the task is 80 s. During 60 s, except for the first and last 10 s, the operator manipulates the baton as instructed by the M-sequence signal. During the first and last 10 s, the baton is not moved from the $x=0$ m position.

In the experiment, the parameters of the impedance model shown in Table 1 are applied to acquire time series data of the iEMG signal and baton velocity when the baton is operated according to the instructions of the M-sequence signal. After data acquisition, the RNN is trained based on Chapter 2.

TABLE I. IMPEDANCE MODEL PARAMETERS EXCLUDING SPRING ELEMENTS.

Parameter	Value
M [kg]	6.0
D [N/(m/s)]	98

C. Results of Hand Velocity Estimation by RNN

Fig. 6 shows the time response of the iEMG signals and hand velocity used to train the RNN. However, the hand velocity data were plotted offset forward by 0.1 s relative to the iEMG signal data. Fig. 7 also shows the time response of the data used for training input to the RNN and the output teaching signal. As shown in Fig. 7, the hand velocity estimates rise and fall in line with the teaching hand velocity, indicating that the RNN was able to learn the relationship between the iEMG signals and the hand velocity. However, even when the teaching hand velocity was near 0 m/s, there were some points where the estimated hand velocity was not near 0 m/s. The reason for this is that the iEMG signals generated by arm stiffness during baton positioning are included in addition to the iEMG signals generated when the baton is moved.

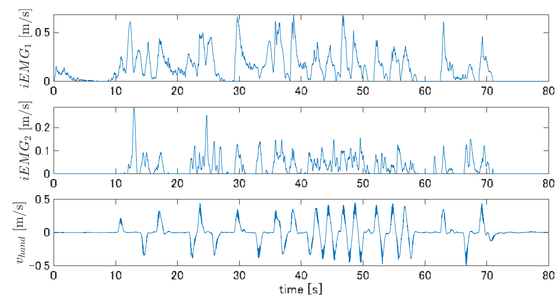

Figure 6. Time response of iEMG signals (feature vector) and hand velocity (teaching signal) used to train RNN: The teaching signal is displayed after shifting by 0.1 seconds earlier to the original time.

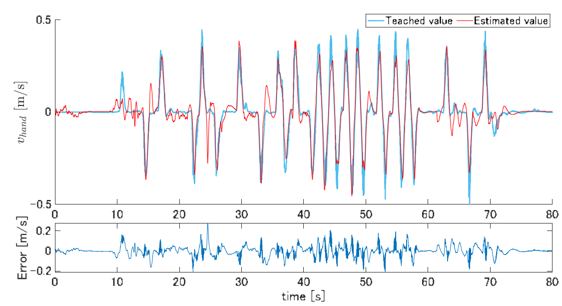

Figure 7. Time responses of estimated hand velocity using training data as input and actual measurement: Since the prediction is made 10 sampling periods ahead, the graph is also plotted and shifted by 10 samples.

D. Selection of Cutoff Frequency for High-pass Filter

This section describes a method for selecting a cutoff frequency for a high-pass filter to prevent drift in the integration of the control system shown in Fig. 1. In the present study, the matching index between human intent and predictive assistive motion was calculated using the forgetting factor based on the exponential function shown in Equation (16) below, and the cutoff frequency was selected to maximize the integral value. Fig. 8 shows the integrated matching index of predictive assistive motion as the cutoff frequency is varied from 0.001 Hz to 1 Hz. As shown in Fig. 8, the integral of the matching index of the predictive assistive motion reaches its maximum value when the cutoff frequency is set to 0.017 Hz. Therefore, the cutoff frequency used in this experiment was set at 0.017 Hz.

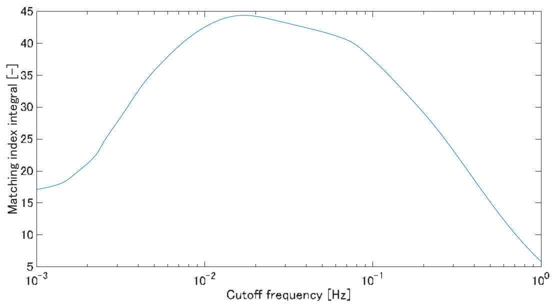

Figure 8. Variation of the integral value of the matching index with respect to the cutoff frequency.

V. Robot Predictive Assistive Motion Experiments Based on Human Hand Velocity Estimates

In this chapter, we describe the experimental results of operating PA10 with the control system shown in Fig. 1, using RNNs trained by the procedure described in Chapter 4.

A. Experimental Conditions and Procedures

In this experiment, the experimental apparatus shown in Fig. 5 in Chapter 4 is used, and the results of the operator's manipulation of the baton with the control system shown in Fig. 1 implemented are described. The predictive assistive motion is performed based on the matching index calculated according to the proposed algorithm. The proposed method is then evaluated by comparing the results of the "human-load index" calculation with the unsupported case.

Specifically, two types of experiments were conducted: one in which the strength of the predictive assistive motion is not adjusted based on the estimated hand velocity (the position command of the predictive assistive motion $\hat{x}_{hand}$ is input 100% as it is) with an adjustment gain $\alpha = 1$, and one in which the strength of the predictive assistive motion is adjusted by calculating an adjustment gain.

Table 2 shows the combination of experimental conditions when adjusting the strength of anticipatory support. As listed in Table. 2， Two methods are available for calculating the adjustment gain , each calculated by

$$\alpha[k] = \frac{r_{x,\hat{x}_{hand}}[k]+1}{2} \tag{12}$$

$$\alpha[k] = \begin{cases} r_{x,\hat{x}_{hand}}[k] & \left(r_{x,\hat{x}_{hand}}[k] \geq 0\right) \\ 0 & \left(r_{x,\hat{x}_{hand}}[k] < 0\right) \end{cases} \tag{13}$$

using the correlation coefficients described in section 3.1. There are two window widths for the matching index calculation, 500 and 200, and three types of forgetting factors: without, linear, and exponential, each defined as shown in

$$g_i = 1 \quad (i = 0 \cdots n-1) \tag{14}$$

$$g_i = \frac{1}{n}(n-i) \quad (i = 0 \cdots n-1) \tag{15}$$

$$g_i = e^{-0.01 i} \quad (i = 0 \cdots n-1) \tag{16}$$

It uses RNNs trained on the data described in Chapter 3. In addition, the parameters of the impedance model use the values shown in Table 1, and the operator manipulates the baton based on the same M-sequence signal instructions as those described in Chapter 4.

To verify the extent to which the load on the operator has been reduced as a measure of the effectiveness of the proposed method, operations with only impedance control implemented without the predictive support are also conducted as a benchmark.

TABLE II. List of combinations of calculation methods of α, window widths, and forgetting factors in experiments.

Calculation method of α	Window width [samples]	Forgetting factor
Based on Equation (12), referred to as No. 1	500	Without
		Liner
		Exponential
	200	Without
		Liner
		Exponential
Based on Equation (13), referred to as No. 2	500	Without
		Liner
		Exponential
	200	Without
		Liner
		Exponential

B. Predictive Assistive Motion Generation Without Coordination

In this section, experimental results are compared with the impedance control alone to evaluate the proposed method when the adjustment gain α and the strength of the predictive assist is not adjusted by the adjustment gain α. However, the forgetting factor used to calculate the matching index is " without".

Fig. 9 shows the results of calculating the matching index between human intent and predictive assistive motion, and Fig. 10 shows the results of calculating human fictitious power. As shown in Fig. 9, the ratio of the positive and negative areas of the matching index is approximately 1.00:0.20, indicating that the area of the negative area is about 20% of the area of the positive area. When the matching index is negative, the actual hand velocity and the velocity of the predictive assistive motion are opposite, indicating that the predictive assistive motion is interfering with the human operation. As shown in Fig. 10, the fictitious power of the human with predictive assistive motion is smaller than that without predictive assistive motion in the 50 s to 60 s region, but the fictitious power is larger in the majority of the regions. The human-load index calculated by integrating the fictitious power shown in Fig. 10 is 176.69 J in the case of impedance control alone without predictive assistive motion and 253.85 J in the case of predictive assistive motion, indicating an increased human-load. The results show that the burden on humans has increased.

From the above, the matching index between human intent and predictive assistive motion is low, and predictive assistive motion interferes with human operation, thus increasing the human-load.

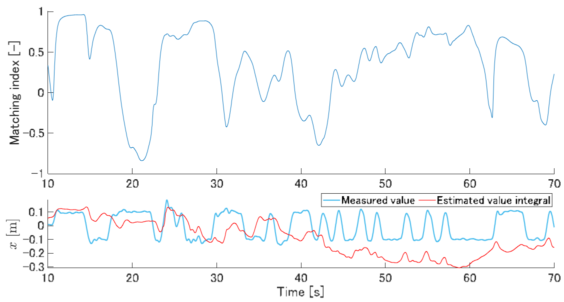

Figure 9. Calculation results of the matching index between human intention and predictive support action (Window width: 500 samples, No forgetting factor used).

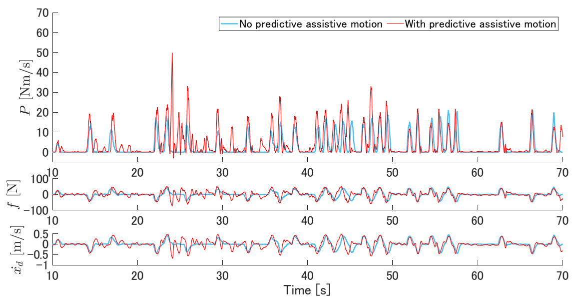

Figure 10. Calculation results of fictitious power of human (Window width: 500 samples, No forgetting factor used).

C. Predictive Assistive Motion Generation with Coordination Based on Adjustment Gain

In this section, the case of adjusting the strength of anticipatory support by adjustment gain is evaluated by comparing it with the case in which only impedance control is implemented and operated as in the previous section. Specifically, the fictitious power is calculated for the experimental results of the manipulation with the strength of anticipatory support adjustment applied by adjustment gain A, and the human-load index is calculated by integrating. The human-load index is compared to the human-load index when the system is operated with only the impedance control implemented, to evaluate how much the human-load is reduced.

Table 3 shows the results of calculating the human-load index for all 12 combinations of conditions shown in Table 2. As shown in Table 3, the human-load index was equivalent to that of impedance control alone only when the window width was 500, the forgetting factor was linear, and the adjustment gain was calculated by the No. 2 (hereinafter referred to as the best combination), but the index was worse under the other conditions. Based on this fact, For the best combination, 10 experiments were conducted under the same conditions, and the human-load index was evaluated. Ten additional experiments were also conducted for the impedance control only case for comparison. These results are shown in Table 4 and Table 5. The human-load index for the implementation of the best combination of the proposed method had a mean value of 229 J and a standard deviation of 7.52 J. In contrast, the human-load index when only impedance control was implemented had a mean value of 257 J and a standard deviation of 16.1 J. To show the validity of the proposed method, a t-test for two samples was conducted assuming that the variances are not equal. Specifically, a one-sided test was conducted to determine whether the human-load index of the proposed method is smaller than that of the impedance control alone. The result showed the p-value of 0.00016, indicating that the effect of the proposed method was significant.

Here, the reasons for the reduction of the human-load index in the best combination are discussed. Fig. 11 shows the time response of the baton position, velocity, and adjustment gain for the best combination (the fourth time in Table 4), and Fig. 12 shows the calculated fictitious power. As shown in Fig. 12, the difference between the actual hand velocity and the estimated hand velocity that would have occurred in the absence of adjustment by adjustment gain α has been eliminated. In areas where the difference between the actual hand velocity and the estimated velocity is small, the adjustment gain is close to 1, indicating that the support based on the estimated velocity of the hand is maintained effectively. As shown in Fig. 12, with predictive assistive motion, the fictitious power is decreased throughout the entire case, although there is an increase in some parts of the fictitious power compared to the case without predictive assistive motion. From the above, the adjustment gains calculated by the best combination can be applied to remove the factors that increase the human-load on the estimated hand velocity and, accordingly, reduce the human-load.

TABLE III. CALCULATION RESULTS OF THE HUMAN-LOAD INDEX FOR EACH CONDITION AS LISTED IN TABLE 2.

Calculation method of α	**Window width**	**Forgetting factor**		
		Without	**Liner**	**Exponential**
No. 1	500	453 J	346 J	393 J
	200	299 J	307 J	287 J
No. 2	500	286 J	264 J	280 J
	200	273 J	299 J	269 J
Only impedance control		265 J		

TABLE IV. CALCULATION RESULTS OF THE HUMAN-LOAD INDEX IN 10 EXPERIMENTS WHEN THE BEST COMBINATION OF THE PROPOSED METHOD IS IMPLEMENTED.

Number of Experiments	**Human-load Index [J]**
1	233
2	243
3	229
4	231
5	224
6	224
7	221
8	237
9	219
10	233
Average	229 J
Standard deviation σ	7.52 J

TABLE V. CALCULATED RESULTS OF HUMAN-LOAD INDEX IN 10 EXPERIMENTS WHEN ONLY IMPEDANCE CONTROL WAS IMPLEMENTED.

Number of Experiments	**Human-load Index [J]**
1	293
2	247
3	255
4	252
5	251
6	272
7	250
8	263
9	248
10	235
Average	257 J
Standard deviation σ	16.1 J

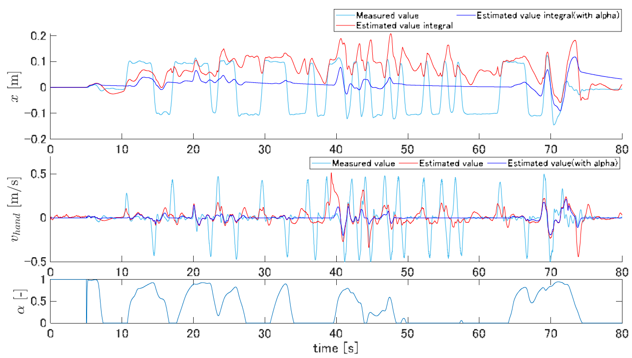

Figure 11. Time response of baton position, velocity and adjustment gain under the best combination of the trial in Table 4.

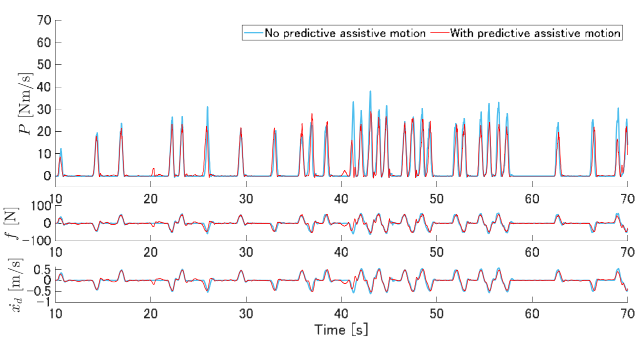

Figure 12. Calculation results of human-load index under the best combination of *the trial in Table 4, compared with no assistive motion.

VI. CONCLUSION

In this section, a concept to realize predictive motion is proposed for a robot that works in cooperation with a human. As a preliminary step to realize the concept, training data acquisition and RNN training and evaluation were conducted. From the training results, it was found that although RNNs hold the features of the teaching signal, there is a difference between the output of RNNs and the teaching signal. The results of the implementation and operation of the proposed method were evaluated using the defined evaluation index. From the results, it was confirmed that when there is a difference between the output of the RNN and the teaching signal, the matching index between the human intent and the predictive assistive motion when implementing the proposed method becomes smaller, and the human-load increases. In contrast, it was confirmed that the human-load can be reduced by adjusting the estimated hand velocity based on the matching index.

REFERENCES

[1] B. Chen, J. Wan, L. Shu, P. Li, M. Mukherjee, and B. Yin, “Smart Factory of Industry 4.0 Key Technologies, Application Case, and Challenges,” *IEEE Access*, vol. 6, pp. 6505–6519 (2018).

[2] O. Onday, “Japan’s Society 5.0: Going Beyond Industry 4.0,” *Business and Economics Journal* (2019).

[3] N. Hogan, “Impedance Control; An Approach to Manipulation, Part I, II, III,” *Proc. of the IEEE International Conference on Robotics Automation*, pp. 1047–1054 (1985).

[4] N. Hogan, “Stable Execution of Contact Tasks Using Impedance Control,” *Proc. of the IEEE International Conference on Robotics Automation*, pp. 1047–1054 (1987).

[5] E. Colgate, N. Hogan, “An analysis of contact instability in terms of passive physical equivalents,” *Proc. of the IEEE International Conference on Robotics Automation*, pp. 404–409 (1989).

[6] F. Dimeas, and N. Aspragathos, “Online Stability in Human Robot Cooperation with Admittance Control,” *IEEE Transactions on Haptics*, vol. 9, no. 2, pp. 267–277 (2016).

[7] K. Kronander, and A. Billard, “Stability Considerations for Variable Impedance Control,” *IEEE Translations on Robotics*, vol. 32, no. 5, pp. 1298–1305 (2016).

[8] B. Khademian, and K. Hashtrudi-Zaad, “A Framework for Unconditional Stability Analysis of Multimaster-Multislave Teleoperation Systems,” *IEEE Translations on Robotics*, vol. 29, no. 3, pp. 684–694 (2013).

[9] G. A. Pratt and M. Williamson, “Series elastic actuators,” *Proc. of the 1995 IEEE/RSJ International Conference on Intelligent Robots and Systems. Human Robot Interaction and Cooperative Robots*, pp. 399–406 (1995).

[10] K. Kong, J. Bae, M. Tomizuka, “Control of Rotary Series Elastic Actuator for Ideal Force-Mode Actuation in Human–Robot Interaction Applications,” *IEEE/ASME Transactions on Mechatronics*, vol. 14, No. 1, pp.105-117 (2009).

[11] K. Kong, J. Bae, M. Tomizuka, “A Compact Rotary Series Elastic Actuator for Human Assistive Systems,” *IEEE/ASME Transactions on Mechatronics*, vol. 17, No. 2, pp.288-297 (2012).

[12] X. Li, Y. Pan, G. Chen, H, Yu, “Adaptive Human–Robot Interaction Control for Robots Driven by Series Elastic Actuators, ” *IEEE/ASME Transactions on Robotics*, vol.33, No.1, pp.169-181 (2017).

[13] J. Rosen, M. Brand, M. B. Fuchs, and M. Arcan, “A myosignal-based powered exoskeleton system,” *IEEE Transactions on Systems, Man, and Cybernetics: Systems-Part A: Systems and Humans*, vol.31, no.3, pp.210–222 (2001).

[14] C. Fleischer and G. Hommel, “A human–exoskeleton interface utilizing electromyography,” *IEEE Transaction on Robotics.*, vol. 24, no. 4, pp. 872–882 (2008).

[15] L. Peternel, T. Noda, T. Petriˇc, A. Ude, J. Morimoto, and J. Babiˇc, “Adaptive control of exoskeleton robots for periodic assistive behaviours based on EMG feedback minimisation,” *PLoS ONE*, vol. 11, no. 2, p. e0148942 (2016).

[16] L. Peternel, N. Tsagarakis, and A. Ajoudani, “A Human-Robot Co-Mnipuration Approach Based on Human Sensorimotor Information”, *IEEE Transactions on Neural System and Rehabilitation Engineering*, vol. 25, no. 7, pp.811-822 (2017).

[17] L. Peternel, T. Petriˇc, E. Oztop, and J. Babiˇc, “Teaching robots to cooperate with humans in dynamic manipulation tasks based on multimodal human-in-the-loop approach,” *Auton Robot*, vol. 36, no. 1, pp.123–136 (2014).